

Modeling of Gaussian beam diffraction on volume Bragg gratings in PTR glass

Igor V. Ciapurin, *Leonid B. Glebov, Vadim I. Smirnov

College of Optics/CREOL, Univ. of Central Florida, P.O. Box 162700, Orlando, FL 32816-2700

ABSTRACT

A detailed model of diffraction of Gaussian beams on plane uniform volume Bragg gratings based on a Kogelnik's theory of coupled waves is presented. The model describes transmitting and reflecting gratings and takes into account spectral width and angular divergence of diffracted beams. Exact formulas for angular and spectral selectivity are derived. Conditions for Bragg diffraction based on comparison between beam quality (divergence and spectral width) and volume grating parameters (angular and spectral selectivity) are formulated. The model results are compared with experimental data for high-efficient Bragg gratings in photo-thermo-refractive (PTR) glass.

Keywords: volume Bragg gratings, numerical approximation and analysis, holographic recording materials, photo-thermo-refractive glass

1 INTRODUCTION

Nowadays volume Bragg gratings (VBGs) are considered as perfect spectral and/or angular selectors with highly adjustable parameters. Angles of incidence and diffraction, central wavelength, and spectral/angular width could be properly chosen by varying of a grating thickness, a period of refractive index modulation, and orientation of grating vector. VBGs are used for spectral beam combining of laser beams with shifted wavelengths,¹⁻³ coupling elements in laser resonators,⁴⁻⁷ beam deflectors, splitters, attenuators, etc. VBGs were recorded in various phase photosensitive media such as photorefractive crystals,⁸⁻¹² dichromated gelatin,^{13,14} photopolymers,¹⁵ and inorganic photosensitive glasses,^{16,17} and used in various configurations. One of the most promising materials for VBGs is a photo-thermo-refractive (PTR) glass which is a silicate one doped with silver, cerium and fluorine.¹⁸ This glass can be used for production of high-efficient holographic elements when both transmitting and reflecting VBGs exhibit diffraction efficiency greater than 95% as well as perfect thermal, optical and mechanical stability in high-power beams were observed.^{19,20} This is why the most important to compare theoretical modeling results with experimental ones obtained for PTR Bragg gratings.

Over the last decades, there are numerous publications on theoretical and experimental studying of volume Bragg gratings. A most widely used basis for description of such gratings is the theory of coupled waves²¹ developed by Kogelnik in 1969. Its results were applied for the further theoretical consideration²²⁻²⁵ and treatment of experimental results observed for VBGs. There are several more approaches describing VBGs, e.g. rigorous coupled-wave analysis²⁶ and beam-propagation method.²⁷ However, Kogelnik's theory is still most used approach for the volume gratings' modeling. The goal of this work is to reduce this rather complicated theory to simple practical formulae which could assist in design of diffractive optics based on volume Bragg gratings. The paper will consider diffraction of plane monochromatic, divergent, and polychromatic laser beams on uniform sinusoidal lossless transmitting and reflecting volume gratings.

2 BASIC DEFINITIONS OF BEAM PROPAGATION AND DIFFRACTION IN BRAGG GRATINGS

A sinusoidal uniform phase grating is a volume structure produced by refractive index modulation as it shown in Fig. 1. Each such structure recorded inside a plane-parallel plate of a photosensitive material could be considered as either

* E-mail address: lbglebov@mail.ucf.edu, phone 407-823-6983, fax 407-823-6880

transmitting or reflecting Bragg grating depending on its orientation in regard to the front surface and wavelength of a readout beam. Fig.1 illustrates a comparison of transmitting and reflecting gratings produced by the same periodical structure in a photosensitive medium. Dotted arrows illustrates the beam tracing in transmitting grating geometry, and dashed arrows - in reflecting one. Solid arrows are the wave vectors of beams and the grating vectors as it is noted in this Figure's caption. In general case, volume Bragg gratings could be entirely described by the following set of parameters: the grating thickness t , an average refractive index of a medium n_{av} , an amplitude of refractive index modulation δn , the grating period Λ (or spatial frequency $f=1/\Lambda$), and the grating inclination angle φ between the normal to the grating front surface N_f and grating vector K_G .

Grating vector K_G is directed as a medium normal to the planes of a constant refractive index and has a module $|K_G|=2\pi f$. It is important to emphasize that a volume sinusoidal grating itself has doubled degeneration of directions of grating vectors due to its symmetry. For example, a volume grating is a transmitting grating for short wavelength radiation with large wave vector which crosses the left vertical surface and directed down to the bottom of the Fig. 1. The same grating is a reflecting one for long wavelength radiation with small wave vector which crosses the bottom surface and the grating vector is directed to the top of this Figure. An inclination angle φ which is the angle between the normal to the front surface N_f and the grating vector K_G , is positive in counter-clockwise direction and can vary from $-\pi/2$ to $+\pi/2$. Transmitting grating excited through the left vertical side of Fig. 1 has negative inclination; the same grating excited through the bottom side is a reflecting grating with positive inclination.

Determination of angles in Bragg gratings is similar to those in classical geometrical optics. Fig. 1 shows an incident beam I_i approaches the front surface of the plate at angle θ_i , refracted into the medium at angle θ_{im} , and diffracted at angle θ_d . For describing of Bragg diffraction in all types of volume gratings regardless of type and inclination, let us introduce an incident Bragg angle in a medium, θ_m^* . This angle is determined as an angle between a grating vector K_G and a wave vector K_i of a refracted beam inside the medium, and it can vary from $-\pi$ to $+\pi$. One can distinguish the following possible cases of Bragg diffraction depicted in Fig. 2. Positive orders of Bragg

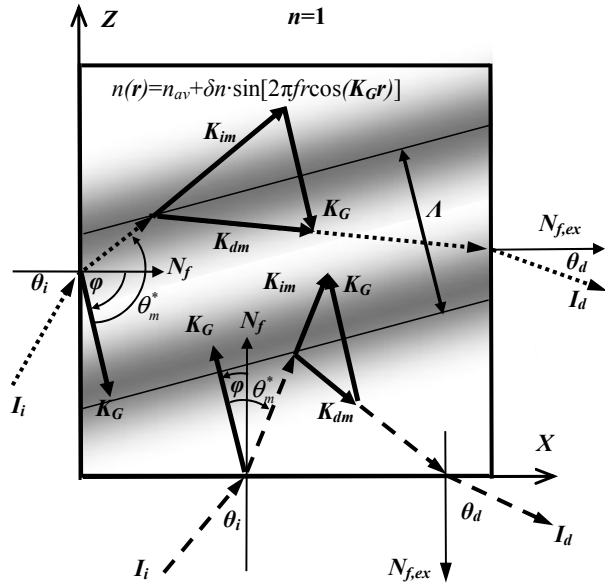


Fig. 1. Propagation of optical rays through a volume Bragg grating. N_f and $N_{f,ex}$ – normals to the front surface for incident (I_i) and diffracted (I_d) beams; K_{im} and K_{dm} – wave vectors of incident and diffracted beams inside the grating medium; K_G – grating vector; φ – grating inclination; θ_i and θ_d – angles of incidence and diffraction; θ_m – Bragg angle; θ_m^* – incident Bragg angle.

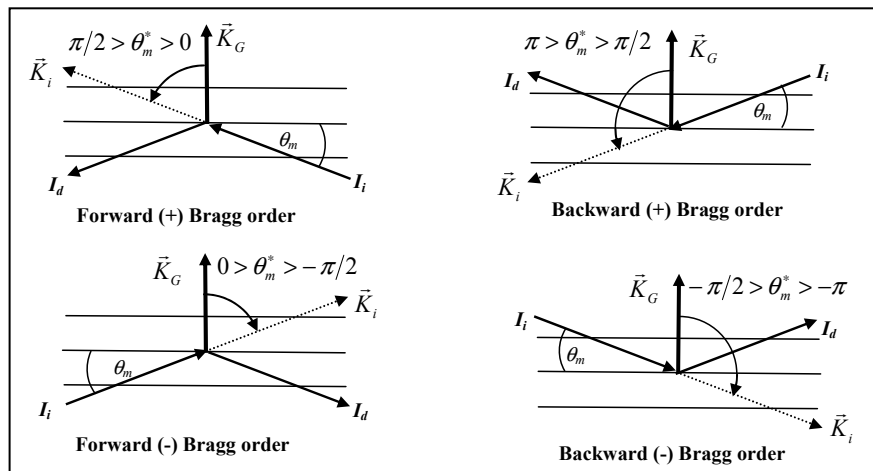


Fig. 2. Possible orders of Bragg diffraction inside medium. I_i and I_d – incident and diffracted beams; K_i – wave vector of incident beam; K_G – grating vector; θ_m – Bragg angle; θ_m^* – incident Bragg angle.

diffraction are for incident Bragg angle ranged from 0 to $+\pi$, i.e. for counter-clockwise direction of an incident beam from grating vector. Similarly, negative orders of Bragg diffraction are for incident Bragg angle ranged from 0 to $-\pi$. The forward orders of Bragg diffraction are for a module of an incident Bragg angle less than $\pi/2$. The backward orders of Bragg diffraction are for a module of an incident Bragg angle more than $\pi/2$. Thus, depending on mutual orientation of grating and incident wave vectors, one can distinguish four Bragg orders, e.g. “plus forward” or “minus backward”, etc.

Traditionally used (beginning from its crystallography applications) conventional Bragg angle in the media θ_m has been determined as a positive angle not exceeding 90° between the plane of a constant refractive index and a direction of the beam propagation. As one can see from Fig. 2, the relationship between a Bragg angle and an incident Bragg angle is $\sin \theta_m = |\cos \theta_m^*|$. It is important to note that θ_m does not describe backward orders of diffraction which are important for practical modeling of volume Bragg gratings.

3. DIFFRACTION OF PLANE MONOCHROMATIC WAVES ON BRAGG GRATINGS

3.1. Transmitting gratings

For volume Bragg gratings, diffraction of a beam with a certain wavelength occurs for the only one certain angle which depends on grating spatial frequency according to Bragg's condition:

$$|\cos \theta_m^*| = \frac{\lambda_0 f}{2n_{av}} \quad (1)$$

In accordance with Kogelnik's theory,²¹ a solution of the scalar wave equation for transmitting VBG gives the following formula for diffraction efficiency (DE):

$$\eta = \frac{\sin^2(\xi^2 + \Phi^2)^{1/2}}{1 + \xi^2/\Phi^2} \quad (2)$$

Here phase incursion Φ is the parameter which determines the maximum diffraction efficiency of VBG (grating strength) when the Bragg condition is obeyed while dephasing parameter ξ describes deviation from the Bragg condition by detuning from either θ_m^* or λ_0 . Phase incursion in Bragg condition could be written as:

$$\Phi = \frac{\pi t \delta n}{\lambda_0 F_\varphi}, \quad (3)$$

where parameter F_φ is an inclination factor:

$$F_\varphi = [-\cos(\varphi - \theta_m^*)\cos(\varphi + \theta_m^*)]^{1/2} \quad (4)$$

For normal transmitting gratings with $\varphi = \pm\pi/2$, the expression for the inclination factor is simplified and becomes:

$$F_{\pi/2} = \sin \theta_m^* = \sqrt{1 - \left(\frac{\lambda_0 f}{2n_{av}}\right)^2}. \quad (5)$$

The inclination factor describes additional optical path of incident and diffracted beams in a medium resulted from deviation of propagation from the normal to the grating surface.

According to Eq. (2), DE of a transmitting grating in Bragg condition ($\xi=0$) is a periodic function of phase incursion Φ and reaches 100% when

$$\Phi = \pi/2 + j\pi, \quad \text{where } j=0, 1, 2, \dots \quad (6)$$

Substitution of this phase incursion to Eq. (3) at $j=0$ and considering a Bragg angle value from Eq. (1) gives a minimum thickness of grating t_0 which provides a 100% DE for a given refractive index modulation δn :

$$t_0 = \frac{\lambda_0 F_\varphi}{2\delta n} \quad (7)$$

Dephasing parameter ξ takes into account small angular deviations $\Delta\theta_m$ from an incident Bragg angle θ_m^* and/or small deviations $\Delta\lambda$ from central wavelength λ_0 :

$$\xi = \frac{\pi f t}{\cos(\varphi - \theta_m^*) - \frac{f \lambda_0}{n_{av}} \cos \varphi} \left(\Delta \theta_m \sin \theta_m^* - \frac{f}{2n_{av}} \Delta \lambda \right) \quad (8)$$

For normal transmitting grating ($\varphi=\pi/2$) this expression is simplified and can be written as:

$$\xi_{\pi/2} = -\pi f t \left(\Delta \theta_m - \frac{f}{2n_{av} F_{\pi/2}} \Delta \lambda \right) \quad (9)$$

Interrelation between spectral and angular parameters could be obtained from differential form of Bragg condition (1):

$$\frac{\Delta \theta_m}{\Delta \lambda} = \frac{f}{2n_{av} F_{\pi/2}} \quad (10)$$

Eq. (10) is universal interrelation between spectral and angular selectivity of VBG that allows easy calculating of one of them from the given (or measured) another.

Angular selectivity of normal transmitting VBGs could be determined by substituting of Eqs (3) and (8) to (2) at $\Delta \lambda=0$:

$$\eta(\Delta \theta_m) = \frac{\sin^2 \left(\pi t \left(\left(\frac{\delta n}{\lambda_0 F_{\pi/2}} \right)^2 + (f \Delta \theta_m)^2 \right)^{1/2} \right)}{1 + \left(\frac{\lambda_0 f F_{\pi/2} \Delta \theta_m}{\delta n} \right)^2} \quad (11)$$

Dependence of diffraction efficiency on detuning from Bragg angle is shown in Fig. 3. Curve 1 corresponds to 2-mm-thick VBG with 250-ppm refractive index modulation which provide 100% diffraction efficiency at 1085 nm. One can see a well known central maximum and a number of side lobes with gradually decreasing magnitude. Curve 2 shows decreasing of DE resulted from decrease of refractive index modulation down to 125 ppm at the same grating thickness; this decreases diffraction efficiency at the central maximum down to 50%, but positions of minima and maxima of the side lobes practically are not changed. Curve 3 shows decreasing of DE resulted from decreasing of the thickness down to 1 mm at $\delta n=250$ ppm; this also provides DE of 50% but it causes dramatic widening of angular selectivity, when the first minimum moves to the position of the second minimum for 2-mm-thick gratings.

It is important to note that Eq. (2) requires the following criterion for equalizing of diffraction efficiency to zero:

$$\left(\xi^2 + \Phi^2 \right)^{1/2} = j\pi, \quad \text{where } j=1, 2, \dots, n, \dots \quad (12)$$

Let us determine angular selectivity inside the VBG medium at the HWFZ (Half Width at First Zero) level, $\delta \theta_m^{HWFZ}$, as the angle between the central maximum and the first minimum at the diffraction efficiency curve. For VBGs with 100% diffraction efficiency the following expression for the HWFZ angular selectivity could be given:

$$\delta \theta_m^{HWFZ} = \frac{\sqrt{3}}{2 f t_0} \approx \frac{0.87}{f t_0} \quad (13)$$

It should be noticed that the HWFZ angular selectivity $\delta \theta_m^{HWFZ}$ is slightly fewer than widely used grating parameter of FWHM angular selectivity which for 100%-efficient grating could be easily estimated as $\delta \theta_m^{FWHM} \approx 1/f t_0$.

By the same way as it was described above for angular selectivity, $\delta \lambda^{HWFZ}$ spectral selectivity is determined as a distance between the central maximum and the first zero in spectral distribution of DE which could be expressed by

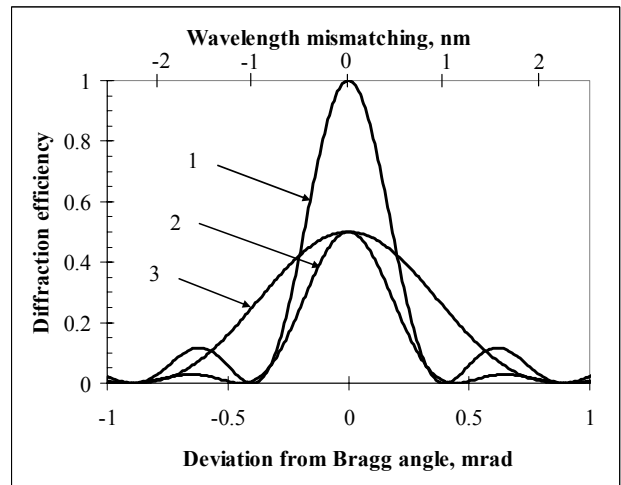


Fig. 3. Selectivity of transmitting Bragg gratings on deviation from Bragg angle and central wavelength for $\lambda_0=1085$ nm, $n_{av}=1.4867$. Grating thickness, mm: 1 and 2 – 2.0, 3 – 1.0. Refractive index modulation, ppm: 1 and 3 – 250, 2 – 125.

substitution of Eqs (3) and (8) to Eq. (2) at $\Delta\theta_m=0$. In the case of normal transmitting grating, this expression is simplified by the use of Eq. (9):

$$\eta(\Delta\lambda) = \frac{\sin^2 \left(\frac{\pi t}{F_{\pi/2}} \left(\left(\frac{\delta n}{\lambda_0} \right)^2 + \left(\frac{f^2 \Delta\lambda}{2n_{av}} \right)^2 \right)^{1/2} \right)}{1 + \left(\frac{f^2 \lambda_0 \Delta\lambda}{2n_{av} \delta n} \right)^2} \quad (14)$$

Spectral selectivity, has the same structure as angular selectivity due to their linear interrelationship described by Eq. (10). For the grating parameters depicted in Fig. 3, this ratio is $\Delta\lambda/\lambda_0 \approx 500 \text{ nm}^{-1}$. Thus, in addition of showing the angular selectivity of 2- and 1-mm-thick transmitting VBGs, Fig. 3 shows spectral selectivity of the same gratings which is represented by the upper horizontal axis of this Figure. For normal transmitting gratings with 100% diffraction efficiency $\delta\lambda^{HWFZ}$ could be derived by substitution of Eq. (13) to Eq. (10):

$$\delta\lambda^{HWFZ} = \frac{\sqrt{3}n_{av}F_{\pi/2}}{f^2 t_0} \quad (15)$$

HWFZ spectral selectivity of transmitting VBG could be easy varied from values below 0.1 nm to more than 100 nm by proper choosing of grating parameters.

3.2. Reflecting gratings

Generally, diffraction efficiency of reflecting Bragg grating is described by the following formula:²¹

$$\eta = \left(1 + \frac{1 - \xi^2 / \Phi^2}{\sinh^2 \sqrt{\Phi^2 - \xi^2}} \right)^{-1} \quad (16)$$

Here Φ and ξ are the same phase incursion at Bragg condition and dephasing parameter at certain detuning from Bragg condition. According to Ref. [21], these parameters should be redefined for reflecting VBG as

$$\Phi = \frac{i\pi t \delta n}{\lambda_0 F_\varphi} \quad (17)$$

$$\xi = \frac{\pi f t}{\cos(\varphi - \theta_m^*) - \frac{f\lambda_0}{n_{av}} \cos\varphi} \left(-\Delta\theta_m \sin\theta_m^* + \frac{f}{2n_{av}} \Delta\lambda \right) \quad (18)$$

For un-slanted reflecting gratings ($\varphi=0$), these parameters becomes

$$\Phi_0 = \frac{\pi t \delta n}{\lambda_0 |\cos\theta_m^*|} = \frac{2\pi n_{av} t \delta n}{\lambda_0^2 f} \quad (19)$$

$$\xi_0 = \frac{\pi f t \Delta\lambda}{\lambda_0} \quad (20)$$

Spectral selectivity could be described in the terms of Bragg grating parameters:

$$\eta(\Delta\lambda) = \left(1 + \frac{1 - \left(\frac{\lambda_0 f^2 \Delta\lambda}{2n_{av} \delta n} \right)^2}{\sinh^2 \left(\left(\frac{2\pi n_{av} t \delta n}{\lambda_0^2 f} \right)^2 - \left(\frac{\pi f t \Delta\lambda}{\lambda_0} \right)^2 \right)^{1/2}} \right)^{-1} \quad (21)$$

Diffraction efficiency of reflecting Bragg grating strongly depends on grating thickness t and refractive index modulation δn . If reflecting VBG is at exact Bragg condition ($\Delta\theta_m = \Delta\lambda = 0$), $\xi=0$, and maximum of the grating diffraction efficiency could be simplified from Eq. (16) as

$$\eta_0 = \tanh^2 \frac{\pi \delta n}{\lambda_0 |\cos \theta_m^*|} \quad (22)$$

Following to the behavior of hyperbolic tangent function, diffraction efficiency maximum asymptotically approaches the 100% value by increasing of grating thickness and/or refractive index modulation. In this case the maximum of grating diffraction efficiency could be predetermined at certain value η_0 which would serve as one more characteristic for reflecting VBG.

Fig. 4 illustrates this interrelation for four different values of diffraction efficiency η_0 : 90% which correspond to 10-dB transmitted-beam-attenuation, 99% (20 dB), 99.9% (30 dB), and 99.99% (40 dB) at $\lambda_0=1085$ nm for normal beam incidence onto a grating. It should be noticed that refractive index modulation δn is less than 1000 ppm only when the grating thickness is more than 1 mm for securing the diffraction efficiency level of $\eta_0=99\%$ (20 dB attenuation). Therefore, reflecting VBGs should be thick enough for securing of their efficient reflection at relatively low values of refractive index modulation.

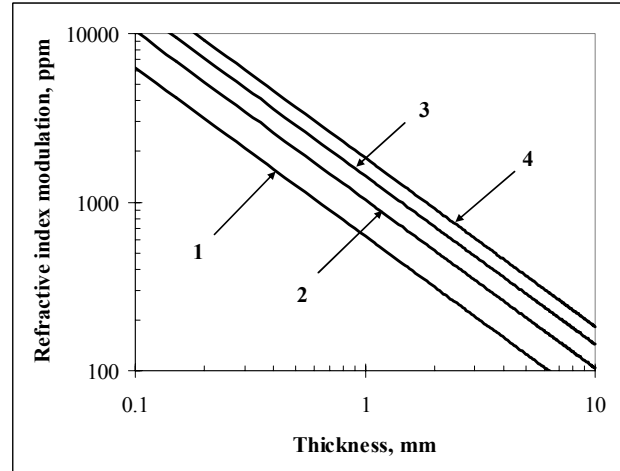


Fig. 4. Dependence of refractive index modulation which secured predetermined diffraction efficiency on the grating thickness. Diffraction efficiency: 1 – 90%, 2 – 99%, 3 – 99.9%, 4 – 99.99%. $\lambda_0=1085$ nm, $n_{av}=1.4867$.

To determine spectral selectivity $\delta\lambda^{HWFZ}$ at HWFZ level, Eq. (25) should be equalized to zero, and diffraction efficiency reaches zero value at multiple points when $\xi \neq \Phi$ (otherwise we have a function singularity at this point):

$$(\xi^2 - \Phi^2)^{1/2} = j\pi, \quad \text{where } j=1, 2, \dots, n, \dots \quad (23)$$

Generally, for determining of spectral selectivity as the HWFZ level, $\delta\lambda^{HWFZ}$, one should substitute Eqs (17) and (18) to (23) at $j=1$. However, this general result could be considerably simplified for un-slanted gratings with diffraction efficiency η_0 :

$$\delta\lambda^{HWFZ} = \frac{\lambda_0 \left((\operatorname{atanh} \sqrt{\eta_0})^2 + \pi^2 \right)^{1/2}}{\pi t} \quad (24)$$

Estimation of typical values of spectral selectivity $\delta\lambda^{HWFZ}$ for $\eta_0=99\%$, $\lambda_0=1085$ nm, $n_{av}=1.485$, and gives the following formula for normal beam incidence:

$$\delta\lambda^{HWFZ} [nm] \cong \frac{0.55}{t [mm]} \quad (25)$$

Let us note that the grating with fixed thickness t exhibits lesser diffraction efficiency η_0 at smaller values δn , and spectral selectivity of such a grating is narrowing, too.

Derivation of the basic interrelation between angular and spectral parameters for reflecting VBG could be performed similarly to the procedure described in Sec. 3.1 for transmitting Bragg gratings. Expression of the Bragg condition, Eq. (1), in its differential form and considering of the second order for angular deviation from exact Bragg angle, one can write the interrelation formula for spectral and angular parameters for reflecting gratings:

$$\Delta\theta_m^{1,2} = \pm \left(\tan^2 \theta_m^* + \frac{2\Delta\lambda}{\lambda_0} \right)^{1/2} + \tan \theta_m^* \quad (26)$$

If we would like to consider angular selectivity at zero level of diffraction efficiency, one can calculate it by substitution of $\Delta\lambda = \delta\lambda^{HWFZ}$ to Eq. (26). However, it defines two different solutions which follows us to introduce two different definitions for angular selectivity shown in Fig. 5. The first one, Full-Width at Zero level angular selectivity, $\delta\theta_m^{FWZ}$, defines as the full distance between two minima (zeros) in angular selectivity that includes both orders of the diffraction efficiency maxima between them:

$$\delta\theta_m^{FWZ} = 2 \left(\tan^2 \theta_m^* + \frac{2\delta\lambda^{HWFZ}}{\lambda_0} \right)^{1/2} \quad (27)$$

By substitution of the spectral selectivity value from Eq. (24), angular selectivity $\delta\theta_m^{FWZ}$ of un-slanted reflecting VBG at predetermined DE value η_0 could be expressed as

$$\delta\theta_m^{FWZ} = 2 \left(\tan^2 \theta_m^* + \frac{2\sqrt{(\operatorname{atanh}\sqrt{\eta_0})^2 + \pi^2}}{\pi ft} \right)^{1/2} \quad (28)$$

Let us note that changing of refractive index modulation (and corresponding changing of grating diffraction efficiency) gradually affects the angular selectivity $\delta\theta_m^{FWZ}$.

When 1-mm-thick VBG has 2000-ppm of refractive index modulation (it corresponds to diffraction efficiency >99.99%), angular selectivity shape changes to total overlapping of diffraction peaks; these peaks are partially separating at $\eta_0 \approx 99.9\%$ ($\delta n = 1500$ ppm) as it is shown in Fig. 5, and then they are fully dividing at $\eta_0 \approx 99\%$ ($\delta n = 1000$ ppm). This result is one of the most important for practical applications of reflecting Bragg gratings because it allows adjusting of grating angular selectivity by changing of the diffraction efficiency near its 100% limit through varying of grating parameters only.

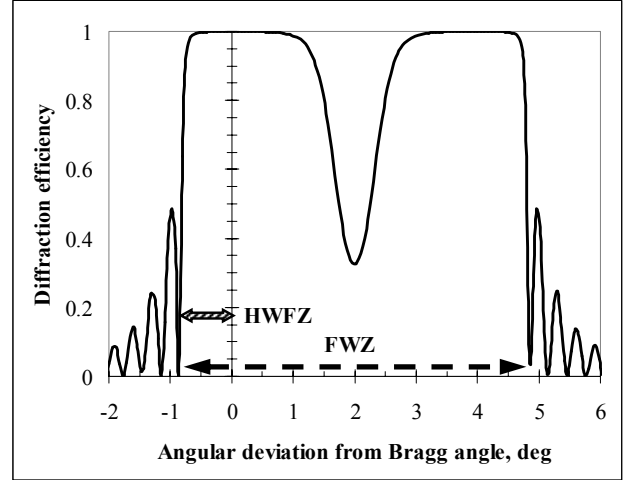


Fig. 5. Definition of angular selectivity at HWFZ (solid arrow) and FWZ (dashed arrow) levels for 1-mm-thick 99.9%-efficient reflecting VBG at incident Bragg angle $\theta_m^* = 2^\circ$. Refractive index modulation $\delta n = 1500$ ppm, $\lambda_0 = 1085$ nm, $n_{av} = 1.4867$.

The second type of angular selectivity at Half-Width at First Zero level, $\delta\theta_m^{HWFZ}$, should be used for practical applications at relatively low diffraction efficiency as well as for higher incident Bragg angles θ_m^* when two diffraction orders don't overlap. HWFZ selectivity determines as an angular distance between the maximum of diffraction efficiency and its first (left) zero in angular selectivity curve:

$$\delta\theta_m^{HWFZ} = |\Delta\theta_m^1| = \left(\tan^2 \theta_m^* + \frac{2\delta\lambda^{HWFZ}}{\lambda_0} \right)^{1/2} - \tan \theta_m^* \quad (29)$$

Let us estimate at what Bragg angle θ_m^* one should consider the HWFZ angular selectivity rather than its FWZ value for a grating with diffraction efficiency η_0 . The criterion to determine this angle, let us call it as a threshold angle θ_0 , might be defined as a incident Bragg angle at which $\delta\theta_m^{FWZ} = 4\delta\theta_m^{HWFZ}$. At all $\theta_m^* < \theta_0$ FWZ selectivity should be used for describing of a grating selectivity, otherwise the doubled value of $\delta\theta_m^{HWFZ}$ should be considered. Combining of Eqs (28) and (29) gives the result:

$$\tan^2 \theta_0 = \frac{2\delta\lambda^{HWFZ}}{3\lambda_0} = \frac{\lambda_0 \left((\operatorname{atanh}\sqrt{\eta_0})^2 + \pi^2 \right)^{1/2}}{3\pi n_{av} t |\cos \theta_0|} \quad (30)$$

Exact solution of Eq. (30) could be expressed as

$$|\cos \theta_0| = \frac{2}{G + \sqrt{G^2 + 4}}, \quad (31)$$

where G is a grating factor which is determined by the grating thickness t and diffraction efficiency η_0 :

$$G = \frac{\lambda_0 \left((\operatorname{atanh}\sqrt{\eta_0})^2 + \pi^2 \right)^{1/2}}{3\pi n_{av} t} \quad (32)$$

Usually G is about 10^{-4} - 10^{-3} ; this defines proximity of $|\cos\theta_0|$ to the unity, and θ_0 is small enough. For $t=1$ mm, $\lambda_0=1085$ nm, and $\eta_0=99\%$, the threshold angle θ_0 is about 1° .

Because there are two different definitions of Bragg grating angular selectivity, one should define at what way the angular selectivity will be determined. At $\theta_m^* < \theta_0$, FWZ angular selectivity is determined by Eq. (28) and showed in Fig. 6(A) for 99%-efficient gratings as a function of incident Bragg angle. One can see, the thicker the grating (in the assumption that all they are 99%-efficient by respective choosing of their refractive index modulation), the higher the HWZ angular selectivity. The angular selectivity $\delta\theta_m^{FWZ}$ is slightly increasing with the increase of the incident Bragg angle; the rate of this increasing is higher for thicker gratings. Fig. 6(B) shows that HWFZ angular selectivity dramatically depends on both incident Bragg angle θ_m^* and VBG thickness t . For instance, 10-mrad HWFZ selectivity is secured at $\theta_m^*=10^\circ$ for 0.3-mm-thick grating, or at $\theta_m^*=2^\circ$ for 1.25-mm grating thickness. One can conclude that reflecting VBG has a minimal angular selectivity near the threshold angle $\theta_0 \approx 1^\circ$.

Hence, despite the fact that spectral selectivity of reflecting Bragg gratings can not be unambiguously specified, one can use one out of two different definitions of angular selectivity in accordance with prevailing of either threshold or incident Bragg angle. This phenomenon is inherent to reflecting Bragg gratings and it could be used for design of high-selective spectral filters with relatively low angular selectivity.

4. DIFFRACTION OF GAUSSIAN BEAMS ON A TRANSMITTING BRAGG GRATING

In this part we present results of Bragg diffraction modeling of monochromatic beam which has the divergence that could be approximated by a Gaussian function. If the direction of the beam propagation matches the Bragg condition, normalized function of the beam intensity in the angular space could be written as

$$G_1(\theta, b) = \exp\left[-2\left(\frac{\theta - \theta_m}{b}\right)^2\right] \quad (33)$$

For diffraction-limited beam with diameter D , the lower the beam diameter, the higher the beam divergence is occurred. For determining of DE of Bragg grating for such divergent beam, convolution in the angular space of the functions given by Eqs (11) and (33) should be applied. After substitution of the numerical value of a Gaussian-function integral, diffraction efficiency could be written as

$$\eta_\theta(b) = \sqrt{\frac{2}{\pi}} \frac{1}{b} \int \eta(\theta) G_1(\theta, b) d\theta \quad (34)$$

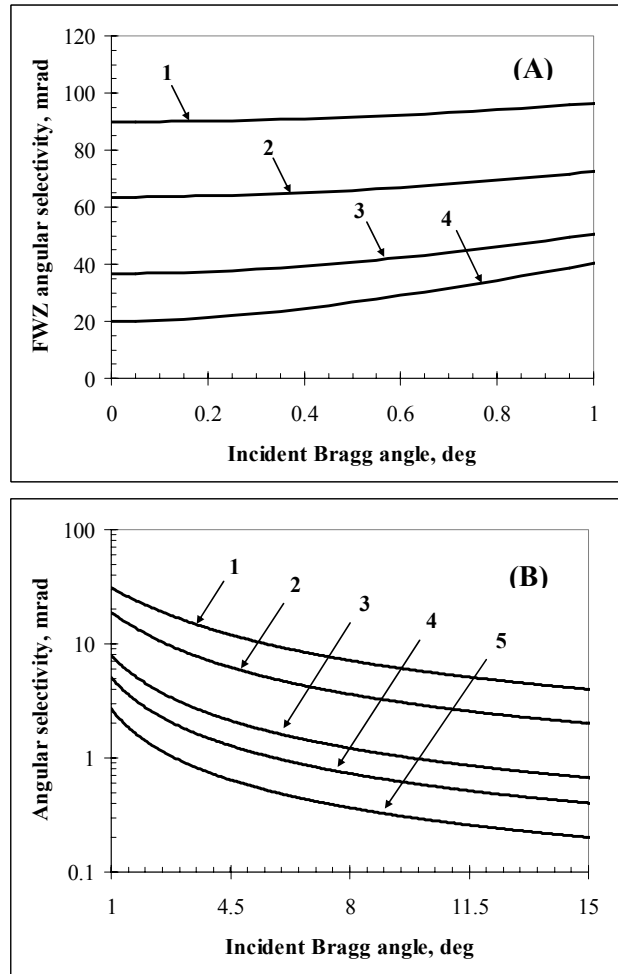


Fig. 6. Dependence of FWZ (A) and HWFZ (B) angular selectivity on incident Bragg angle for 99%-efficient reflecting VBG at $\lambda_0=1085$ nm, $n_{av}=1.4867$. Grating thickness, mm: (A) - 1 - 0.5; 2 - 1.0; 3 - 5.0; 4 - 10. (B) - 1 - 0.5; 2 - 1.0; 3 - 3.0; 4 - 5.0; 5 - 10.

Fig. 7(A) shows angular selectivity of the grating with $\delta\theta_m^{HWFZ}=0.4$ mrad and 100% diffraction efficiency for a plane monochromatic wave at 1085 nm for four beams with different divergences b . While the beam divergence is much less than the grating angular selectivity (Curve 1 corresponding $b=0.04$ mrad), there is no decrease of diffraction efficiency compare to that for planar wave and the curve minima reach zero values as it appears for the planar wave (Fig. 3). However, if the beam divergence becomes comparable with the grating selectivity, dramatic decreasing of maximal DE occurs (Curves 2-4). When divergence and selectivity values are equal, $b=\delta\theta_m^{HWFZ}$, maximum diffraction efficiency is about 60% only. Also, side lobes are flattening while the divergence increasing, local minima of angular selectivity starting to differ from zero significantly, and at $b\geq\delta\theta_m^{HWFZ}=0.4$ mrad the selectivity curve does not have any local minima at all.

Fig. 7(B) shows the dependence of diffraction efficiency on the beam divergence. Four gratings with thickness 20 and 2.0 mm and spatial frequency 357 mm^{-1} as well as with thickness 2.0 and 0.2 mm and spatial frequency 1086 mm^{-1} have respective values of HWFZ angular selectivity of 0.12, 1.2, 0.4, and 4 mrad in accordance with Eq. (13). It was found that diffraction of a divergent beam causes decreasing of diffraction efficiency down to 99% when the beam divergence b becomes 8 times less than the grating HWFZ angular selectivity $\delta\theta_m^{HWFZ}$, i.e. losses are less than 1% when $8b\leq\delta\theta_m^{HWFZ}$. Further increasing of the beam divergence b (e.g. by decreasing of the beam diameter for diffraction-limited beams) results in dramatic decreasing of the DE value. When the beam divergence is equal to the grating angular selectivity $\delta\theta_m^{HWFZ}$, diffraction efficiency decreases almost twice (down to 58%).

If we consider the Bragg diffraction of polychromatic beams with Gaussian shape of the spectral distribution:

$$G_2(\lambda, w) = \exp\left[-2\left(\frac{\lambda - \lambda_0}{w}\right)^2\right], \quad (35)$$

where parameter w is the HWe^{-2}M spectral width and λ_0 is a central wavelength of a beam. Modeling of such diffraction could be performed similarly as it was done for divergent beams. Diffraction efficiency of transmitting VBG for such beams could be calculated from convolution of the DE for monochromatic wave determined by Eq. (15) with the Gaussian spectral distribution described by Eq. (35). This gives us the adjusted value of diffraction efficiency $\eta_\lambda(w)$:

$$\eta_\lambda(w) = \sqrt{\frac{2}{\pi}} \frac{1}{w} \int \eta(\lambda) G_2(\lambda, w) d\lambda \quad (36)$$

Again, taking into account spectral-angular reciprocity in accordance with Eq. (10), one can conclude that the grating DE is only about 60% when the beam spectral width w is equal to the grating selectivity $\delta\lambda^{HWFZ}$. Diffraction efficiency

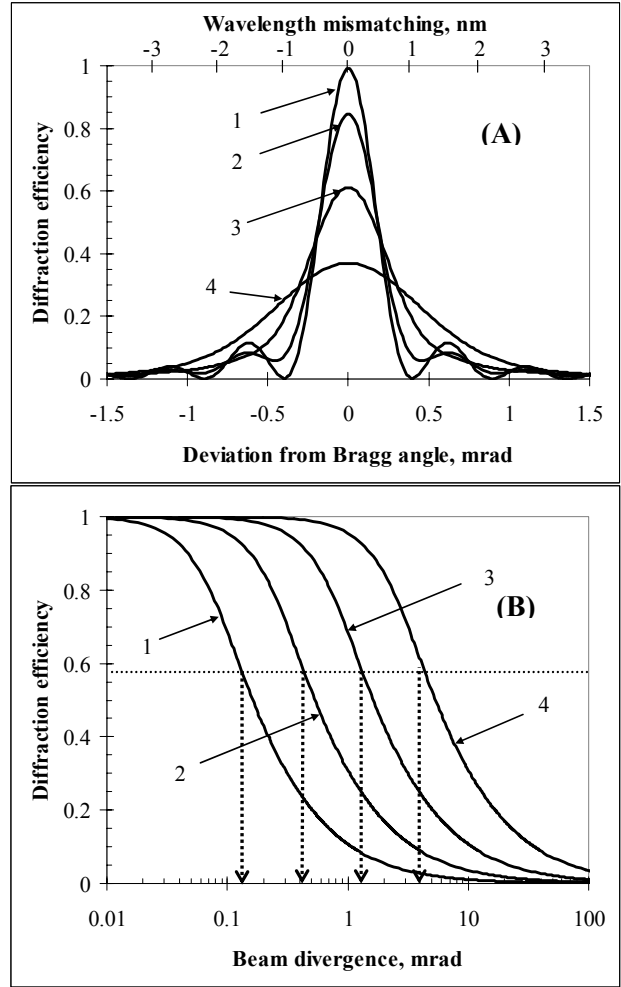


Fig. 7. Selectivity of transmitting VBG for divergent beams. (A) - Dependence of diffraction efficiency on detuning from Bragg angle. Beam divergence, mrad: 1 – 0.04, 2 – 0.2, 3 – 0.4, 4 – 0.8; grating angular selectivity is 0.4 mrad. (B) - Dependence of grating DE on the beam divergence. Grating angular selectivity, mrad: 1 – 0.12, 2 – 0.4, 3 – 1.2, 4 – 4.0; shown by dotted arrows. Dotted line corresponds to diffraction efficiency for a beam with divergence or spectral width equal to the grating selectivity.

for narrow-spectral-line beams is the same as for monochromatic wave, and it is decreasing down to 99% when beam spectral width becomes approximately 8 times fewer than the grating HWFZ spectral selectivity, i.e. when $\delta\lambda^{HWFZ}=8w$.

5. DIFFRACTION OF GAUSSIAN BEAMS ON A REFLECTING BRAGG GRATING

Similarly to diffraction of Gaussian beams on transmitting Bragg gratings described above, we will consider the Bragg diffraction by comparing of grating selectivity with the beam spectral width and/or angular divergence. Results of numerical calculations of Bragg diffraction on reflecting gratings are shown in Fig. 8. Fig. 8(A) shows how different polychromatic beams diffract on 1.1-mm-thick grating which has DE=99% at normal beam incidence. According to Eq. (24), this VBG has 0.5-nm-spectral selectivity. One can see that diffraction efficiency drops down while beam spectral widening; this grating has diffraction efficiency of about 60% when $w=2\delta\lambda^{HWFZ}$. In comparison with the same dependence of spectral selectivity for transmitting gratings described above, when 60%-level of DE achieved at $w=\delta\lambda^{HWFZ}$, one can conclude that spectral width of incident beams is twice less restrictive parameter for reflecting VBGs in comparison with the transmitting ones. Also, side lobes in the spectral selectivity curves are beginning to disappear when the beam spectral width is approximately twice less than the grating spectral selectivity ($2w\geq\delta\lambda^{HWFZ}$); total flattening of the DE curve occurs when these values become equal each to other and for further increasing of the beam spectral line-width ($w\geq\delta\lambda^{HWFZ}$).

Fig. 8(B) shows dependence of diffraction efficiency $\eta_\lambda(w)$ on the beam spectral bandwidth w for a set of VBG with different spectral selectivity. These gratings have thickness of 10.9, 5.5, 1.1, and 0.55 mm, and all they are 99%-efficient for monochromatic wave. Their spectral selectivity is determined from Eq. (27) as 0.05, 0.1, 0.5, and 1.0 nm, respectively. One can see that 99%-efficient reflecting VBG exhibits fewer losses in the DE value in comparison with 100%-efficient transmitting VBG when a beam bandwidth is equal to spectral selectivity of the grating. In this case, only about 10% from the diffraction efficiency for monochromatic beam becomes lost. There is no considerable decreasing in gratings' DE for the narrowest beams, and the decreasing from 99% to 98% occurs when beam width w becomes approximately twice less than the grating spectral selectivity. This parameter for 1%-efficiency-decreasing ratio is about 4 times less restrictive in comparison with the same parameter for transmitting VBG as it was determined above in Sec. 4.

It is important to note that the general shape of the curves showed in Fig. 8 does not change when the beam incidence is not normal (i.e. incident Bragg angle $\theta_m^* \neq 0$) but the central beam wavelength obeys the relation $\lambda_0 = \lambda_0^{\max} |\cos\theta_m^*|$. Thus one can use the criterion described above for determining of diffraction losses resulting from spectral widening of diffracted beams for all values of incident Bragg angles θ_m^* .

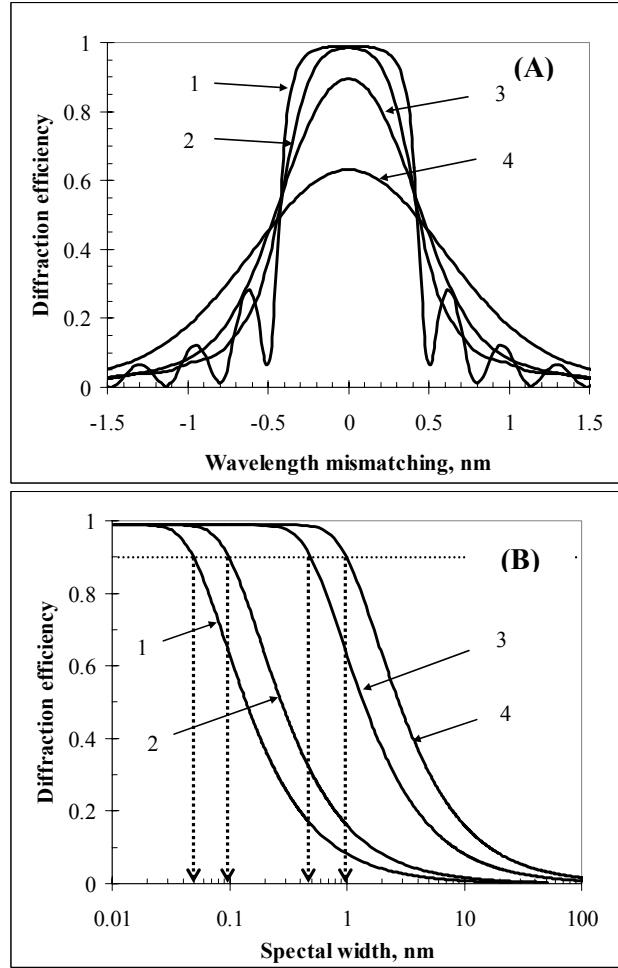


Fig. 8. Selectivity of 99%-efficient reflecting VBG for polychromatic plane waves at normal incidence. (A) - Dependence of diffraction efficiency on spectral mismatching from Bragg condition. Beam spectral width, nm: 1 – 0.05, 2 – 0.25, 3 – 0.5, 4 – 1.0; grating Spectral selectivity is 0.5 nm. (B) - Dependence of grating DE on the beam spectral width. Grating spectral selectivity, nm: 1 – 0.05, 2 – 0.1, 3 – 0.5, 4 – 1.0; shown by dotted arrows. Dotted line corresponds to diffraction efficiency for a beam with spectral width which is equal to the grating selectivity.

Although the general shape of angular selectivity for reflecting VBG at normal incidence is the same as its spectral selectivity shown in Fig. 8, two different values of angular selectivity described above determines slightly different interrelations between grating selectivity, beam divergence, and resulting diffraction efficiency. The main difference is in reaching of a local maximum in characteristic value of diffraction efficiency (which corresponds to equilibrium of HWFZ grating selectivity to beam divergence) at $DE \approx 95\%$ for $\theta_m^* = \theta_0$ due to overlapping of positive and negative diffraction orders. Further increasing of incident Bragg angle results in weak decreasing of this DE value down to about 90%-level; it is in good correlation with the data shown in Fig. 8 for spectral selectivity. Generally, reflecting VBGs are less restrictive for securing of high DE in comparison with transmitting VBGs, especially for divergent beams at the incident Bragg angle near threshold one, but they have higher spectral selectivity which could considerably restrict efficient Bragg diffraction of wide-spectrum beams.

6. COMPARISON OF THE MODEL AND EXPERIMENTAL RESULTS

To prove the model experimentally, we recorded transmitting VBG in 1.23-mm-thick PTR glass with spatial frequency of 425 mm^{-1} and refractive index modulation of 420 ppm which should exhibit $DE=100\%$ for planar monochromatic wave at 1085 nm. 100-W CW single-mode Yb-doped fiber laser (IPG Photonics Corp., model YLR-100) with central wavelength of 1085 nm was used for testing. This laser had collimated output (5-mm-diameter Gaussian beam). This laser has near-diffraction-limited divergence of 0.23 mrad in the whole studied power region while spectral width at the $HW_{e^{-2}M}$ level increases from 2.7 to 4.7 nm, when the output power rose from 15 to 100 W.

Dependence of DE of PTR Bragg grating on the laser power is shown in Fig. 9. Because PTR Bragg gratings have no thermally induced effects at power density levels up to 100 kW/cm^2 , DE decreasing could be explained by changing of laser beam parameters at different levels of emitting power. Based on theoretical modeling results, we evaluated how spectral width and divergence of the beam affect diffraction efficiency of this particular grating. Theoretical DE of this grating is expected to be equal to 100% for planar monochromatic wave. Diffraction of the laser beam with 0.23-mrad-divergence on the grating with angular selectivity of 1.6 mrad (HWFZ) results in decreasing of diffraction efficiency down to 98.6% (Line 1). For planar polychromatic wave with spectral width linearly increasing with power increase, calculated diffraction efficiency dependence on power is shown as Line 2. Line 3, as a result of multiplication of Lines 1 and 2, presents the calculated DE for polychromatic divergent beam which should drop down from 93.5 to 87% for beams with spectral width of 2.7 nm and 4.7 nm, respectively. Corresponding experimental data are 93 and 87% (triangles in Fig. 9). Comparison of calculation data with experimental results shows very good correspondence. Thus, the proposed model is able to describe diffraction of polychromatic divergent beams on real PTR Bragg gratings. Another consequence of this coincidence is that the experimental PTR Bragg grating is very close sinusoidal uniform grating as it was supposed in the model.

7. CONCLUSIONS

- Practical mathematical model based on Kogelnik's coupled wave theory is developed for diffraction of Gaussian beams with wide range of spectral width and angular divergence.
- The model allows fast analytical calculation and could be used for design of different devices based on volume Bragg grating and testing tools for Bragg grating certification.

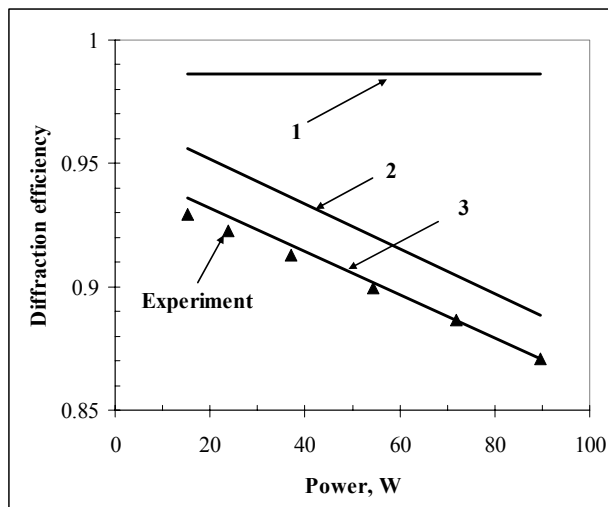


Fig. 9. Dependence of diffraction efficiency of PTR Bragg grating on power of radiation with central wavelength at 1085 nm. Triangles – experimental results. 1 – DE calculation for monochromatic beam with 0.2-mrad-divergence. 2 – DE calculation for planar wave with spectral width equal to the experimental values, 3 – product of 1 and 2.

- Requirements for parameters of gratings and laser beams for lossless Bragg diffraction are formulated.
- Theoretical model is compared with and found very close to experimental data.

ACKNOWLEDGMENT

The work has been supported by the AFRL contract # F49620-01-1-0469.

REFERENCES

1. I. V. Ciapurin, L. B. Glebov, and V. I. Smirnov, in *Fiber Lasers: Technology, Systems, and Applications*, L.N. Durvasula, Ed., Proc. SPIE, **5335**, 216 (2004).
2. I. V. Ciapurin, V. I. Smirnov, G. B. Venus, L. N. Glebova, E. V. Rotari, and L. B. Glebov, *2004 CLEO/QECC and PhAST Technical Digest*, Paper CTuP51 (2004).
3. M. S. Shahriar, J. Riccobono, M. Kleinschmit, and J. T. Shen, *Opt. Comm.* **220**, 75 (2003).
4. G. B. Venus, V. I. Smirnov, and L. B. Glebov, *17th Annual Solid State and Diode Laser Technology Review (SSDLTR-2004) Technical Digest*, Paper Poster-14 (2004).
5. B. L. Volodin, S. V. Dolgy, E. D. Melnik, E. Downs, J. Shaw, and V. S. Ban, *2004 OFC Technical Digest*, Paper WC2 (2004).
6. S. Yiou, F. Balembois, P. Georges, and J. Huignard, *Opt. Lett.* **28**, 242 (2003).
7. A. Dergachev, P. F. Moulton, V. I. Smirnov, and L. B. Glebov, *2004 CLEO/QECC and PhAST Technical Digest*, Paper CThZ3 (2004).
8. Robert T. B. James, Christopher Wah, Keigo Iizuka, and Hiroshi Shimotahira, C.-C. Sun, M.-S. Tsaur, and B. Wang, *Opt. Eng.* **38**(9) 1567 (1999).
9. J.-W. An, N. Kim, and K.-W. Lee, *Opt. Commun.* **197**, 247 (2001).
10. Ph. Dittrich, G. Montemezzani, and P. Gunter, "Tunable optical filter for wavelength division multiplexing using dynamic interband photorefractive gratings", *Opt. Commun.* **214**, 363-370 (2002).
11. V. M. Petrov, S. Lichtenberg, A. V. Chamrai, J. Petter, and T. Tschudi, *Thin Solid Films* **450** 178 (2004).
12. J. Zhou, W. Tang, and D. Liu, *Opt. Commun.* **196**, 77 (2001).
13. J.-H. Chen, D.-C. Su, and J.-C. Su, *Appl. Phys. Lett.* **81**(8), 1387 (2002).
14. J. J. Butler, M. A. Rodriguez, M. S. Malcuit, and T. W. Stone, *Opt. Commun.* **155**, 23 (1998).
15. V. A. Borgman, L. B. Glebov, et al., *Sov. Phys. Dokl.* **34**, 1011 (1989).
16. L. B. Glebov, N. V. Nikonov, et al., *Opt. Spectrosc.* **73**, 237 (1992).
17. O. M. Efimov, L. B. Glebov, L. N. Glebova, and V. I. Smirnov. "Process for production of high efficiency volume diffractive elements in photo-thermo-refractive glass," *United States Patent* 6,586,141 (2003).
18. L. B. Glebov, V. I. Smirnov, C. M. Stickley, I. V. Ciapurin, in *Laser Weapons Technology III*, W. E. Thompson and P. H. Merritt, Eds., Proc. SPIE, **4724**, 101 (2002).
19. O. M. Efimov, L. B. Glebov, and V. I. Smirnov, "High efficiency volume diffractive elements in photo-thermo-refractive glass," *United States Patent* 6,673,497 (2004).
20. H. Kogelnik, "Coupled wave theory for thick hologram gratings", *Bell Syst. Tech. J.* **48**, 2909 (1969).
21. M. W. McCall, *Math. and Comp. Modeling* **34**, 1483 (2001).
22. M. R. Chatterjee and D. D. Reagan, *Opt. Eng.* **38**(7), 1113 (1999).
23. T. Erdogan, *Opt. Comm.* **157**, 249 (1998).
24. J. Zhao, P. Yeh, M. Khoshnevisan, and I. McMichael, *J. Opt. Soc. Am. B* **17**(6), 898 (2000).
25. M. G. Moharam, T. K. Gaylord, *J. Opt. Soc. Am.* **71**, 811 (1981).
26. D. Yevick, L. Thylen, *J. Opt. Soc. Am.* **72**, 1084 (1982).